

CFD Modeling of Traffic-related Air Pollution in Street Canyon

M. Biliaiev¹, V. Biliaieva², O. Berlov³, V. A. Kozachyna⁴, V. V. Kozachyna⁵, Z. Yakubovska⁶

¹Ukrainian State University of Science and Technologies, Lazaryan Str. 2, 49010, Dnipro, Ukraine, E-mail: biliaiev.m@gmail.com

²Ukrainian State University of Science and Technologies, Lazaryan Str. 2, 49010, Dnipro, Ukraine, E-mail: yikabelyaeva604@gmail.com

³Ukrainian State University of Science and Technologies, Lazaryan Str. 2, 49010, Dnipro, Ukraine, E-mail: berlov.oleksandr@pdaba.edu.ua

⁴Ukrainian State University of Science and Technologies, Lazaryan Str. 2, 49010, Dnipro, Ukraine, E-mail: v.kozachyna@gmail.com

⁵Ukrainian State University of Science and Technologies, Lazaryan Str. 2, 49010, Dnipro, Ukraine, E-mail: tsurkanvaleri1997@gmail.com

⁶Ukrainian State University of Science and Technologies, Lazaryan Str. 2, 49010, Dnipro, Ukraine, E-mail: zinaidaya25@gmail.com

<https://doi.org/10.5755/e01.2351-7034.2024.P120-125>

Abstract

High pollution levels are often observed in urban street canyons. Different mathematical models are intensively used to predict pollution levels in urban street canyons. In this paper quick computing 3D CFD model is proposed to compute wind flow over buildings and pollutant dispersion in street canyon. To simulate wind flow over buildings 3D equation of potential flow has been used. Pollutant concentration field has been modelled using three-dimensional equation of pollutant dispersion. Governing equations are also included simplified equations to describe pollutants chemical transformations in atmosphere. To solve numerically governing equations implicit difference schemes have been used. The computer code to realize the proposed numerical models has been developed. Results of numerical experiments are presented.

KEY WORDS: *auto transport, street canyon, air pollution modeling, numerical simulation*

1. Introduction

Motor vehicles are the largest source of air pollution (Fig. 1). In addition, there is a rapid trend of increasing number of automobiles in different countries in the world. For this reason, interest in the development of theoretical methods for assessing the impact of motor vehicles has increased significantly [1-6]. The use of such methods has a certain advantage over the method of physical modeling, which requires large material costs and time to organize and conduct the experiment, both in laboratory and field conditions. Empirical and analytical models allow to promptly obtain data on the possible level of atmospheric air pollution. However, their significant disadvantage is that they do not take into account the presence of buildings when obtaining forecast estimates.



Fig. 1 Emissions from motor vehicles (<https://cutt.ly/8ee7Vcl5>)

In this connection, there is an increased interest in the development of numerical models to study the processes of atmosphere air pollution by motor transport emissions. For practice it is important to have fast numerical models that allow to perform a set of forecast calculations during a working day.

2. Mathematical Model

Numerical integration of modeling equations was carried out by the method of finite difference schemes. Markers

(porosity technique) were used to form a view of the computational region (Fig. 2) [8]. These markers allowed to separate computational cells where the numerical integration of governing equations was carried out from the finite difference cells which corresponded to buildings. Markers also allowed to form the position of the road, the emission rate from cars at the different parts of the road.

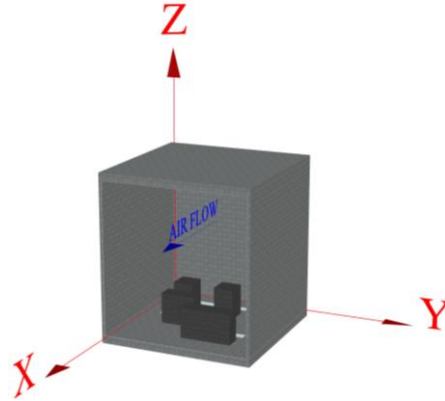


Fig. 2 Sketch of calculation region

Markers allowed to form very quickly the "geometry" of the computational region, i.e. the position of buildings, their shape.

To simulate air flow over buildings Eq. (1) for velocity potential was used:

$$\frac{\partial^2 P}{\partial x^2} + \frac{\partial^2 P}{\partial y^2} + \frac{\partial^2 P}{\partial z^2} = 0, \quad (1)$$

where P – velocity potential.

Boundary conditions for Eq. (1) are considered in [8].

Wind speed components were determined as follows:

$$u = \frac{\partial P}{\partial x}, v = \frac{\partial P}{\partial y}, w = \frac{\partial P}{\partial z}.$$

For numerical integration of Eq. (1), the alternating-triangle method was used. To use this method, Eq. (1) for the velocity potential was written in the form:

$$\frac{\partial P}{\partial t} = \frac{\partial^2 P}{\partial x^2} + \frac{\partial^2 P}{\partial y^2} + \frac{\partial^2 P}{\partial z^2}, \quad (2)$$

where t – fictitious time. For $t \rightarrow \infty$ the solution of Eq. (2) will tend to "steady" solution, i.e. to the solution of Eq. (1).

The two-steps change-triangle method was used for numerical integration Eq. (2). These steps of splitting were as follows:

- first step:

$$\begin{aligned} \frac{P_{i,j,k}^{n+1/2} - P_{i,j,k}^n}{0.5\Delta t} = & \frac{P_{i+1,j,k}^n - P_{i,j,k}^n}{\Delta x^2} + \frac{-P_{i,j,k}^{n+\frac{1}{2}} + P_{i-1,j,k}^{n+\frac{1}{2}}}{\Delta x^2} + \\ & + \frac{P_{i,j+1,k}^n - P_{i,j,k}^n}{\Delta y^2} + \frac{-P_{i,j,k}^{n+\frac{1}{2}} + P_{i,j-1,k}^{n+\frac{1}{2}}}{\Delta y^2} + \\ & + \frac{P_{i,j,k+1}^n - P_{i,j,k}^n}{\Delta z^2} + \frac{-P_{i,j,k}^{n+\frac{1}{2}} + P_{i,j,k-1}^{n+\frac{1}{2}}}{\Delta z^2}; \end{aligned}$$

- second step:

$$\begin{aligned} \frac{P_{i,j,k}^{n+1} - P_{i,j,k}^{n+1/2}}{0.5\Delta t} &= \frac{P_{i+1,j}^{n+1} - P_{i,j}^{n+1}}{\Delta x^2} + \frac{-P_{i,j}^{n+1/2} + P_{i-1,j}^{n+1/2}}{\Delta x^2} + \\ &+ \frac{P_{i,j+1,k}^{n+1} - P_{i,j,k}^{n+1}}{\Delta y^2} + \frac{-P_{i,j,k}^{n+1/2} + P_{i,j-1,k}^{n+1/2}}{\Delta y^2} + \\ &+ \frac{P_{i,j,k+1}^{n+1} - P_{i,j,k}^{n+1}}{\Delta z^2} + \frac{-P_{i,j,k}^{n+1/2} + P_{i,j,k-1}^{n+1/2}}{\Delta z^2}. \end{aligned}$$

At each step, the velocity potential was calculated at the centers of the difference cells using an explicit formula. The calculation was over when the following condition was fulfilled:

$$\left| P_{ijk}^{n+1} - P_{ijk}^n \right| \leq \varepsilon,$$

where ε – a small number ($\varepsilon = 0.001$); n – iteration number.

After calculation of the velocity potential field, the components of the air flow velocity vector were calculated according to the dependencies:

$$u_{ijk} = \frac{P_{i,j,k} - P_{i-1,j,k}}{\Delta x}, v_{ijk} = \frac{P_{i,j,k} - P_{i,j-1,k}}{\Delta y}, w_{ijk} = \frac{P_{i,j,k} - P_{i,j,k-1}}{\Delta z}.$$

Pollutant dispersion process was modeled using Eq. (3):

$$\begin{aligned} \frac{\partial C}{\partial t} + \frac{\partial uC}{\partial x} + \frac{\partial vC}{\partial y} + \frac{\partial (w - w_g)C}{\partial z} &= \\ = \frac{\partial}{\partial x} \left(\mu_x \frac{\partial C}{\partial x} \right) + \frac{\partial}{\partial y} \left(\mu_y \frac{\partial C}{\partial y} \right) + \frac{\partial}{\partial z} \left(\mu_z \frac{\partial C}{\partial z} \right) &+ \\ + \sum Q_i(t) \delta(x - x_i) \delta(x - y_i) \delta(x - z_i), & \end{aligned} \quad (3)$$

where $C(x, y, z, t)$ – concentration of pollutant (NO , NO_2 or O_3), g/m^3 ; u, v, w – components of the air flow velocity vector, m/s ; μ_x, μ_y, μ_z – diffusion coefficients, m^2/s ; w_g – gravity fallout speed, m/s ; t – time, s ; $Q_i(t)$ – emission rate of pollutant at the road, g/s ; x_i, y_i, z_i – coordinates of pollutant emission, m ; $\delta(x-x_i)\delta(y-y_i)\delta(z-z_i)$ – Dirac delta functions, m^{-1} .

Boundary conditions and initial condition for Eq. (3) are considered in [8].

The wind profile at the inlet boundary and diffusion coefficients in the computational region were calculated by formulas:

$$u = u_1 \cdot (z/z_1)^{n_1};$$

$$\mu_x = k_0 \cdot u, \mu_y = k_0 \cdot v, \mu_z = k_1 \left(\frac{z}{z_1} \right)^m.$$

where u_1 – wind speed at height $y_1 = 10$ m; $k_1 = 0.1$; $m \approx 1$; $n_1 = 0.15$; $k_0 = 0.2$.

To solve numerically Eq. (3) method of splitting was used. Splitting was performed as follows:

$$\frac{\partial C}{\partial t} + \frac{\partial wC}{\partial z} = \frac{\partial}{\partial z} \left(\mu_z \frac{\partial C}{\partial z} \right); \quad (4)$$

$$\frac{\partial C}{\partial t} + \frac{\partial uC}{\partial x} + \frac{\partial vC}{\partial y} = \frac{\partial}{\partial x} \left(\mu_x \frac{\partial C}{\partial x} \right) + \frac{\partial}{\partial y} \left(\mu_y \frac{\partial C}{\partial y} \right); \quad (5)$$

$$\frac{\partial C}{\partial t} = \sum Q_i(t) \delta(x - x_i) \delta(x - y_i) \delta(x - z_i). \quad (6)$$

Here was assumed $w = w - w_g$.

For numerical integration of Eq. (4), the following change-triangle difference scheme was used:

- first step of splitting:

$$C_{ijk}^{n+\frac{1}{2}} = C_{ijk}^n - \Delta t \frac{w_{i+1,jk}^+ C_{ijk}^{n+\frac{1}{2}} - w_{ijk}^+ C_{i-1,j,k}^{n+\frac{1}{2}}}{\Delta z} + \Delta t \mu_z \frac{-C_{ijk}^{n+\frac{1}{2}} + C_{i-1,jk}^{n+\frac{1}{2}}}{\Delta z^2} + \Delta t \mu_z \frac{-C_{ijk}^n + C_{i+1,jk}^n}{\Delta z^2};$$

- second step of splitting:

$$C_{ijk}^{n+1} = C_{ijk}^{n+\frac{1}{2}} - \Delta t \frac{w_{i+1,jk}^- C_{i+1,jk}^{n+1} - w_{ijk}^- C_{ijk}^{n+1}}{\Delta z} + \Delta t \mu_z \frac{-C_{ijk}^{n+\frac{1}{2}} + C_{i-1,jk}^{n+\frac{1}{2}}}{\Delta z^2} + \Delta t \mu_z \frac{-C_{ijk}^{n+1} + C_{i+1,jk}^{n+1}}{\Delta z^2}.$$

At each step of splitting, the unknown value of the pollutant concentration was determined by an explicit formula. For the numerical integration of Eq. (5), its physical splitting was performed as follows:

$$\frac{\partial C}{\partial t} + \frac{\partial uC}{\partial x} + \frac{\partial vC}{\partial y} = 0; \quad (7)$$

$$\frac{\partial C}{\partial t} = \frac{\partial}{\partial x} \left(\mu_x \frac{\partial C}{\partial x} \right) + \frac{\partial}{\partial y} \left(\mu_y \frac{\partial C}{\partial y} \right). \quad (8)$$

Further, the following difference splitting schemes were used:

1. For numerical solving Eq. (7), a two-step splitting scheme was used:

- first step:

$$\frac{C_{i,j,k}^k - C_{i,j,k}^n}{\Delta t} + L_x^+ C^k + L_y^+ C^k = 0;$$

- second step:

$$\frac{C_{i,j,k}^{n+1} - C_{i,j,k}^k}{\Delta t} + L_x^- C^{n+1} + L_y^- C^{n+1} = 0.$$

For the numerical solution of Eq. (8):

$$\frac{C_{i,j,k}^{n+\frac{1}{2}} - C_{i,j,k}^n}{\Delta t} = \left[\mu_x \frac{-C_{i,j,k}^{n+\frac{1}{2}} + C_{i-1,j,k}^{n+\frac{1}{2}}}{\Delta x^2} \right] + \left[\mu_y \frac{-C_{i,j,k}^{n+\frac{1}{2}} + C_{i,j-1,k}^{n+\frac{1}{2}}}{\Delta y^2} \right],$$

$$\frac{C_{i,j,k}^{n+1} - C_{i,j,k}^{n+\frac{1}{2}}}{\Delta t} = \left[\mu_x \frac{C_{i+1,j,k}^{n+1} - C_{i,j,k}^{n+1}}{\Delta x^2} \right] + \left[\mu_y \frac{C_{i,j+1,k}^{n+1} - C_{i,j,k}^{n+1}}{\Delta y^2} \right].$$

Notation of difference operators $L_x^+, L_x^-, L_y^+, \dots$ is given in [8]. In these splitting schemes, at each step, the unknown value of pollutant concentration was determined by an explicit formula. To solve Eq. (6) Euler's method was used.

To simulate chemical transformations of pollutants the following equations were used [3]:

$$\begin{aligned} \frac{\partial C_{NO}}{\partial t} &= -k_3 \cdot C_{NO} \cdot C_{O_3} - k_{12} \cdot C_{NO}; \\ \frac{\partial C_{NO_2}}{\partial t} &= -J_T \cdot C_{NO_2} + k_3 \cdot C_{NO} \cdot C_{O_3} + k_{12} C_{NO}; \\ \frac{\partial C_{O_3}}{\partial t} &= J_T \cdot C_{NO_2} - k_3 \cdot C_{NO} \cdot C_{O_3}, \end{aligned}$$

where $J_T = 0.461$ [1/h], $k_{12} = 1.7927$ [1/h], $k_3 = 0.00152$ [ppb⁻¹ h⁻¹] [3].

To solve equations of chemical transformations Euler's method was used.

On the basis of the considered numerical model computer code was developed.

3. Results

Developed CFD model was used to simulate air pollution between complex of buildings which were situated near the road. Location of the road and its configuration is shown in Fig. 3 and Fig.5 by red color. There were 4 buildings in the computational region. Numerical experiment was carried out for the following initial data: dimension of computational region – 600 m×300 m×160 m; the height of buildings 32 m; $u_1 = 4.5$ m/s.

Example simulation result is shown in Figs. 3-6. These Figures present NO concentration at 19 m and 34 m above the surface. Fig. 3 and Fig. 5 show concentration in dimensionless form: each number in these Figures show the concentration as the percentage of the maximum concentration in this section. This approach allows quickly understand where the most intensive pollution takes place. Fig. 4 and Fig. 6 show isolines of concentration in computational region at two different levels above the surface.

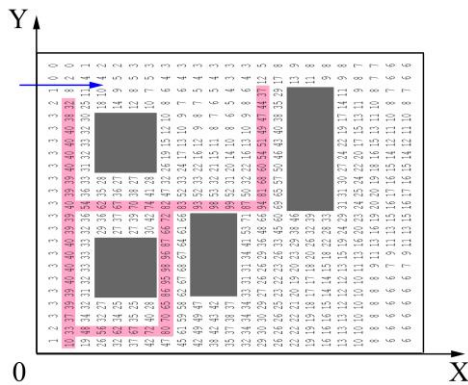


Fig. 3 Concentration (dimensionless) in section $z = 19$ m

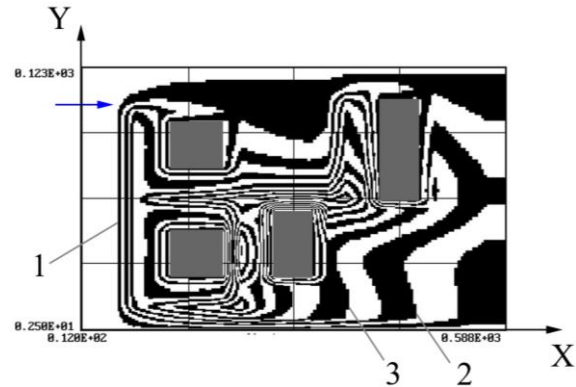


Fig. 4 Isolines of concentration in section $z = 19$ m:
1 – $C = 0.42$ mg/m³; 2 – $C = 0.97$ mg/m³;
3 – $C = 1.54$ mg/m³

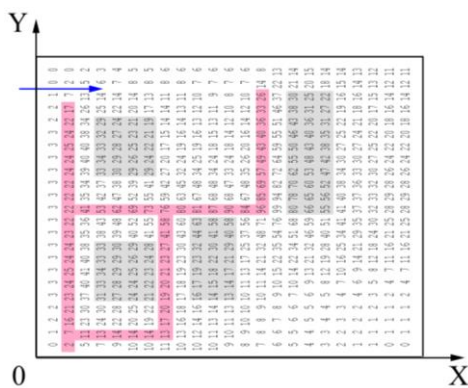


Fig. 5 Concentration (dimensionless) in section $z = 32$ m

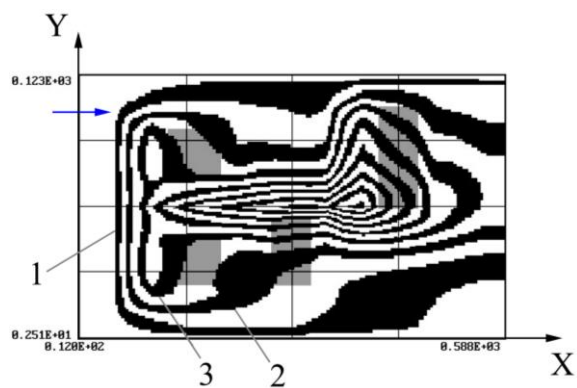


Fig. 6 Isolines of concentration in section $z = 32$ m: 1 – $C = 0.21$ mg/m³; 2 – $C = 0.48$ mg/m³;
3 – $C = 0.76$ mg/m³

Results of numerical experiment show that the buildings play a key role in the distribution of pollutant in the street (Fig. 3., Fig. 4). At the level which is above the buildings (Fig. 5, Fig. 6) this influence of buildings is less and the picture of pollutant distribution is like a "vague" picture. From Figures it is evident that the region with high concentration gradient is formed in canyon between buildings. In this region concentration is in the range 62–99% of maximum concentration.

Worthy of note that computational time was 7 sec.

4. Conclusions

An efficient 3-D CFD model was proposed for calculating pollutant concentration field in urban areas like a street canyon with heavy traffic flow pass. This model allows to take into account: dimensions of buildings, their geometrical form and location, position of road, rate of vehicle emissions, non uniform wind speed pattern in the region. The model allows to compute quickly air flow pattern over buildings, that is the most time-consuming mathematical problem. This flow pattern is used to compute pollutant dispersion from vehicles among the buildings. Computational calculations were carried out on the basis of the developed program "CANYON-3", the computing time was about 7 s.

The developed 3-D CFD model can be used for air quality management in street canyons.

References

1. **Biliaiev, M.; Pshinko, O.; Rusakova, T.; Biliaieva, V.; Sladkowski, A.** 2021. Computer Model for Simulation of Pollutant Dispersion Near the Road with Solid Barriers, *Transport Problems* 16(2)Part 1: 73-86.
2. **Steinberga, I.; Sustere, L.; Bikse, J., Bikse, J.Jr.; Kleperis, J.** 2019. Traffic induced air pollution modeling: scenario analysis for air quality management in street canyon, *Procedia Computer Science* 149: 384-389.
3. **Overman, H.T.** 2009. Simulation model for NO_x distribution in a street canyon with air purifying pavement. Master thesis, University Twente, Netherlands: 99 p.
4. **Tajdaran, S.; Bonatesta, F.; Mason, B.; Morrey, D.** 2022. Simulation of traffic-born pollutant dispersion and personal exposure using high-resolution computational fluid dynamics, *Environments* 9(6):1-16.
5. **Sathe, Y.V.** 2012. Air Quality Modeling in Street Canyons of Kolhapur City, *Universal Journal of Environmental Research and Technologies* 2(2): 97-105.
6. **Shuo-Jun, Me.; Zhiwen, L.; Fu-Yun, Z.; Han-Qing, W.** 2019. Street canyon ventilation and airborne pollutant dispersion: 2-D versus 3-D CFD simulations, *Sustainable Cities and Society*, 50.
7. **Fu, X.; Liu, J.; Ban-Weiss, G. A.; Zhang, J.; Huang, X.; Ouyang, B.; Popoola, O.; Tao, S.** 2017. Effects of canyon geometry on the distribution of traffic-related air pollution in a large urban area: Implications of a multi-canyon air pollution dispersion model, *Atmospheric environment* 165: 111-121.
8. **Zgurovsky, M.Z.; Skopetsky, V.V.; Khrutch, V.K.; Biliaiev, M.M.** 1997. Numerical modeling of pollution dispersion in environment. Kyiv: Naukova dumka, 368 p.